

## Aerodynamic Performance Investigation on a Co-rotating Scroll Hydrogen Recirculation Pump for Fuel Cell Engines

Han WANG<sup>1</sup>, Panpan SONG<sup>2\*</sup>, Mingshan WEI<sup>3</sup>, Ding WU<sup>4</sup>, Zhenbo LU<sup>5</sup>, Zhongyan AN<sup>6</sup>

School of Mechanical Engineering, Beijing Institute of Technology, No. 5 South Zhongguancun Street, Haidian, Beijing 100081

### ABSTRACT

The hydrogen recirculation pump is the core component of the hydrogen supply system of the vehicle fuel cell engine. This paper innovatively put forward a conceptual design of a high-speed co-rotating array scroll hydrogen recirculation pump with the fixed radial sealing position to ensure easy sealing on radial clearance leakage and without the dynamic balance weight. The array scroll structure has advantages in reducing the radial size and could significantly improve the pumping efficiency and realize the compact and lightweight design.

The parametric design of the hydrogen recirculation pump was carried out. Then the aerodynamic performance of the hydrogen recirculation pump was analyzed via the three-dimensional unsteady numerical simulation with the advanced and effective dynamic mesh technology combining morphing and remeshing functions. Firstly, the transient flow field characteristics in the scroll hydrogen recirculation pump under the design operating condition were investigated. Secondly, the effects of rotating speed on performance parameters such as mass flow rate and isentropic efficiency of hydrogen recirculation pump were analyzed. Finally, the study focused on the effects of hydrogen humidity on the aerodynamic performance of the designed co-rotating scroll hydrogen recirculation pump.

The results show that the fluid in the compression chamber is low-speed, and the turbulence at the inlet of the suction chamber and the central exhaust chamber is intense. For the co-rotating hydrogen recirculation pump, the increase of speed will not only aggravate the gap leakage but also aggravate the over-compression phenomenon, resulting in the increase of exhaust loss as well as a decrease of isentropic efficiency at high speed. The highest isentropic efficiency occurs at the design

speed, which is 84.31%. The humidity of hydrogen has a certain effect on aerodynamic performance. Compared with dry hydrogen, the isentropic efficiency decreases by 2.3% at 100% humidity, but the pressure and temperature rise change lightly, increasing by 0.63Kpa and decreasing by 0.3k respectively. Different hydrogen humidity has a great influence on the flow rate. With the increase of humidity, the gap flow velocity at the same rotating angle decreases by about 30m/s.

**Keywords:** Fuel cell, hydrogen recirculation pump, co-rotating scroll, array scroll, aerodynamic performance, hydrogen humidity

### NOMENCLATURE

<i>Abbreviations</i>	
MFR	Mass Flow Rate
<i>Symbols</i>	
$R_b$	Base circle radius
$\alpha$	Initial angle of the scroll
$\Phi_s$	Starting angle of the scroll
$\Phi_e$	Ending angle of the scroll
$R_{or}$	Eccentricity
$C_r$	Radial clearance
$h$	Scroll height
$t$	The thickness of the scroll
$P_t$	Pitch
$D_m$	Maximum circumscribed circle diameter
$N$	Rotating speed
$P_i$	Inlet pressure
$P_o$	Outlet pressure
$T_i$	Inlet temperature
$\omega$	Humidity of hydrogen

## 1. INTRODUCTION

With the acceleration of the development and utilization of clean energy, the hydrogen fuel cell vehicle industry based on the development of hydrogen energy would flourish. As the core component of the hydrogen supply system of hydrogen fuel cell vehicles, the hydrogen recirculation pump directly affects the stable and reliable operation of the hydrogen fuel cell. At present, the hydrogen circulation pumps are mainly roots-type, claw-type, and centrifugal type. Roots-type is reliable, but the volumetric efficiency is greatly affected by pressure ratio, and the backflow is severe at a high-pressure ratio<sup>[1]</sup>. The Claw pump has slight vibration and low noise, but its internal leakage is serious<sup>[2]</sup>. The Centrifugal hydrogen pump has a compact structure, but has low efficiency and is easy to surge<sup>[3]</sup>. Compared with these types, the scroll hydrogen recirculation pump has significant advantages such as high efficiency, low noise, and vibration. However, the scroll hydrogen recirculation pump still has the problem of the large radial size of the whole machine on large displacement occasions, which is difficult to overcome with the traditional structure of one pair of scrolls.

To achieve the design goal of large displacement and compactness, the present paper proposed a co-rotating array scroll hydrogen recirculation pump. Compared with the structure of one pair of scrolls, the radial size can be reduced by using the array scroll structure under the same displacement<sup>[4]</sup>, which has been applied in the design of scroll air compressor<sup>[5]</sup> and scroll vacuum pump<sup>[6]</sup>. In terms of motion mode, compared with the eccentric orbiting of the orbiting scroll, the co-rotation mode of the scroll can allow higher rotation speed, further improve the displacement and reduce the volume. In addition, since the centrifugal inertia force generated by the eccentric orbiting motion of the orbiting scroll does not exist in the co-rotation mode, no balance weight is needed<sup>[7]</sup>. As a result, the drive shaft can be shorter and lighter, which is conducive to the lightweight design of the pump.

At present, the research on co-rotating scroll machines mainly focuses on the application of different scenarios and structural design. Luis Eric Olmedo et al.<sup>[8]</sup> studied and optimized the co-rotating type scroll expander used in the organic Rankine cycle, and showed that the efficiency of oil-lubricated scroll expander reached 80%. In the application of air energy storage, Luis Mendoza Toledo et al.<sup>[9-11]</sup> designed and built a co-rotating scroll machine that can be used as a compressor or expander. The machine tests were carried out with

water injection and non-water injection conditions. In terms of structural design, Robert W. Shaffer<sup>[12]</sup> proposed the co-rotating scroll with idler shaft. John P.D. Wilson<sup>[13]</sup> used two motors to drive two volutes respectively through gear transmission and puts forward the concept of dual-drive co-rotating spinning scroll compressor or expander.

To analyze the aerodynamic performance of the scroll hydrogen recirculation pump, CFD numerical simulation is needed. However, there are few numerical simulations on the co-rotating scroll hydrogen recirculation pump, especially for the array scroll structure. In addition, few numerical simulations of the wet hydrogen compression pumping process were considered. Based on the parametric design of the hydrogen pump structure, this paper carried out a three-dimensional unsteady numerical simulation using the morphing and remeshing dynamic grid technology to study the pump aerodynamic performance. Also, considering the influence of different water vapor ratios, this paper compared and analyzed the performance differences of co-rotating scroll hydrogen recirculation pump with the hydrogen of different humidity as working fluid.

## 2. DESIGN OF CO-ROTATING SCROLL HYDROGEN RECIRCULATION PUMP

### 2.1 Working principle

For a co-rotating hydrogen recirculation pump with two pairs of scrolls, there are two same scrolls with a phase difference of 180 degrees on each scroll plate. Figure 1 shows the pumping process of hydrogen in a working chamber represented by symbol V. Two offset plates rotate synchronously around their rotating axis in the same direction. The recirculated exhaust hydrogen is gradually compressed with the reduction of the working chamber volume. The discharge process begins when the scrolls disengaged downstream of the minimum compression chamber. The hydrogen with low pressure is continuously pumped in the next revolution.

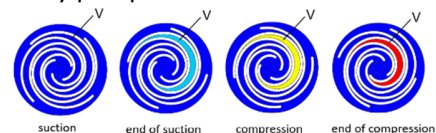


Fig. 1. Working process

### 2.2 Parametric design

According to the requirement of the hydrogen supply in a 50kW fuel cell engine, the scroll geometry was designed. The inlet and outlet pressure of the pump is

0.16Mpa and 0.18Mpa, the inlet temperature is 350K, and the inlet hydrogen volume flow of 336NL/min. Table 1 shows the scroll parameters of the co-rotating hydrogen recirculation pump with two pairs of scrolls at 10000rpm, which were obtained by the program iterative design method.

Table 1

Parameter	Value
$R_b$ /mm	2.89
$\alpha$ /rad	0.38
$\Phi_s$ /rad	2.82
$\Phi_e$ /rad	11.36
$R_{or}$ /mm	2.3
$C_r$ /mm	0.04
$h$ /mm	21.5
$t$ /mm	2.2
$P_t$ /mm	9.08
$D_m$ /mm	81.72

### 3. NUMERICAL METHOD

#### 3.1 Geometry and meshing

Based on the design results, the simplified model of co-rotating hydrogen recirculation pump with two pairs of scrolls is shown in Figure 2 (a) and (b). As is shown in Figure 3, polygonal Mesher and Prism Layer Mesher were used to mesh the inlet and outlet pipe and fluid domain.

As an advanced dynamic grid technology, morphing and remeshing were employed to control the mesh quality as the position of the scroll boundary changes with the rotation. Within a certain number of steps, morphing is used to control the deformation and sliding of the grid nodes to adapt to the boundary movement. To avoid negative volume mesh, remeshing will monitor the overall mesh quality and trigger mesh reconstruction when the mesh quality is lower than a specific limit. The generated mesh could be saved for the first revolution. There is no need to repeat meshing operations in the following revolutions.

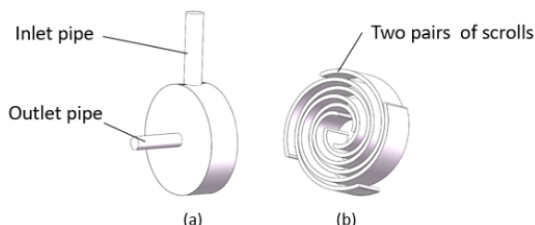


Fig. 2. Simplified geometric model

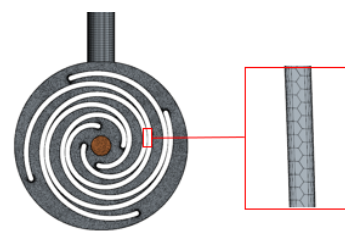


Fig. 3. Meshing

#### 3.2 Turbulence model and boundary conditions

The ideal gas model is used to simulate both the dry hydrogen and wet hydrogen, and the compression process is assumed to be approximately adiabatic. Due to the accurate simulation for vortex and boundary layer flow, the turbulence model Realizable K- $\epsilon$  was employed to reflect the internal flow state of the scroll hydrogen recirculation pump. For the region closed to the scroll wall where the turbulence flow is not fully developed, the Two-Layer All  $y^+$  Wall Treatment method was used. The boundaries of stagnation inlet and pressure outlet were selected for the inlet and outlet of the simulation model, respectively. Table 2 shows the simulation condition of the co-rotating scroll hydrogen recirculation pump.

Table 2

Simulation condition				
N /rpm	10000			
Pi /Mpa	0.16			
Ti /K	350			
Po /Mpa	0.18			
$\omega$ /%	0	20	60	100

#### 3.3 Grid independence verification

Four levels of the grid with different numbers were used to verify the mesh independence. As shown in Figure 4, the isentropic efficiency of the scroll hydrogen recirculation pump has no noticeable change with the increase of the number of grids when the grid number is larger than 1026762. The third level with grid number 1300396 was finally selected for the simulation model.

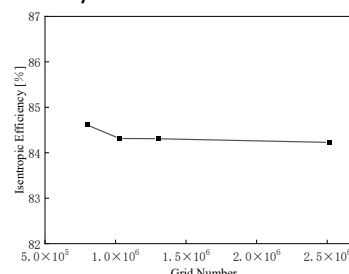


Fig. 4. Grid independence verification

## 4. RESULTS AND DISCUSSION

### 4.1 Flow field characteristics

#### 4.1.1 Pressure distribution

Figure 5 (a)~(f) shows the change of pressure in a working process where  $V_s$ ,  $V_c$ , and  $V_d$  represent the processes of suction, compression, and discharge. With the rotation of the main shaft, the pressure in the working chamber at the end of compression exceeded the design discharge pressure, resulting in over compression. As shown in Figure 5 (d) and (f), the obvious compression phenomenon exists. The pressure at the end of compression reaches 1.99bar, while the pressure in the central discharge chamber is equal to the design discharge pressure of 1.8bar.

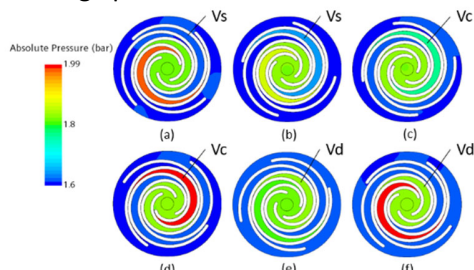


Fig. 5. Pressure change with rotation angle

#### 4.1.2 Velocity distribution

The velocity field distribution at different rotation angles from 90 to 360 degrees and Mach number distribution at 360 degrees are shown in Figure 6 (a). The high-speed fluid is concentrated at the suction and discharge region, while the fluid flow in the compression chamber is in a low-speed state. Volumetric compression with a low speed of fluid flow indicates a high compression efficiency. Due to the sequential discharge determined by the structure of the arrayed scrolls, a high-speed vortex in the central discharge region affects the discharge flow in the axial direction. The maximum Mach number is about 0.114, regarded as incompressible flow.

Under the influence of boundary motion and pressure gradient, the fluid velocity distribution in different working chambers has its characteristics. Under the influence of wall shear force and extrusion, the fluid velocity in the compression chamber presents an S-shaped distribution. The inlet section of the suction chamber and the outlet section of the exhaust chamber are affected by the inlet high-speed fluid and pressure gradient, respectively, and the fluid velocity direction is relatively consistent. In contrast, the S-shaped velocity direction distribution is still present in the middle section, as shown in Figure 6 (b).

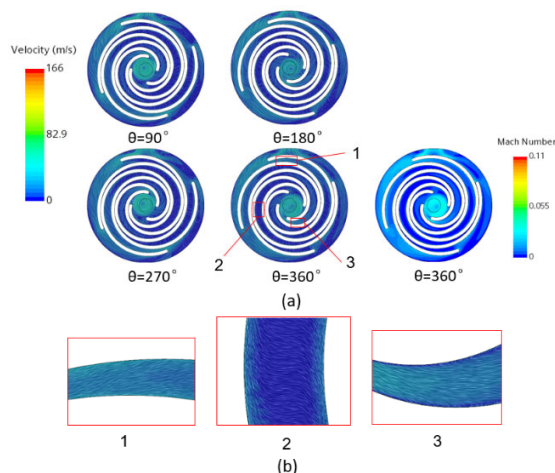


Fig. 6. Velocity field

#### 4.1.3 Turbulence distribution

Figure 7 shows the distribution of Turbulent Kinetic Energy at 90 degrees. The regions with intense turbulence developed are concentrated at the suction and central discharge region. Different scrolls block the suction in sequence at different rotation angles near the tail of the scroll, where the high-intensity turbulence occurs. The rotation of scrolls affects fluid flow in the central discharge chamber continuously and largely, resulting in the highest Turbulent Kinetic Energy. Figure 8 shows that the suction and discharge mass flow rate fluctuates four times in one revolution. The discharge mass flow rate fluctuation is significantly greater than that of suction.

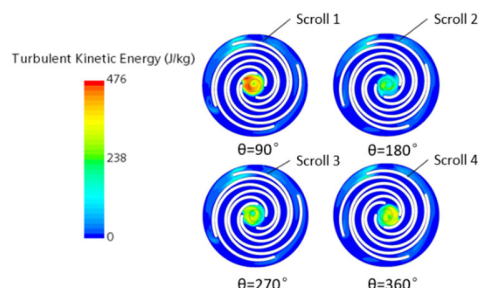


Fig. 7. Distribution of Turbulent Kinetic Energy

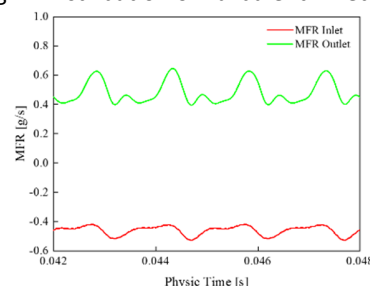


Fig. 8. Mass flow rate fluctuation

#### 4.1.4 Entropy distribution

The entropy distribution at the four typical positions is similar. There is an apparent entropy increasing at the

radical clearance. The entropy and corresponding pressure distribution at 360 °rotation angle are shown in Figure 9 (a). The entropy increases obviously at position 1 and 2 of the radical clearance. The clearance leakage from the high-pressure chamber to low pressure shown in Figure 9 (b) will lead to fluid mixing, resulting in apparent entropy increasing upstream of the clearance. Compared with the pressure distribution, it can be seen that the entropy increasing at position 2 is not caused by the leakage from high pressure to low pressure. There is only a pressure difference of less than 0.1bar between the two adjacent working chambers. The effect of the inverse pressure gradient is not apparent, while the central vortex and wall shear forces play a leading role in the increase of entropy.

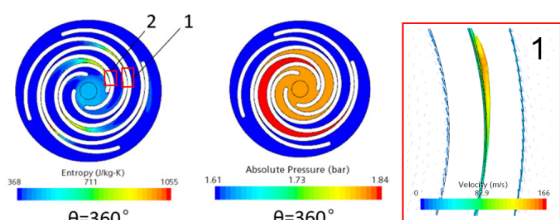


Fig. 9. Velocity field

#### 4.2 Effect of rotating speed on the pump performance

The changes in mass flow and isentropic efficiency under different rotating speeds are shown in Figure 10. With the increase of rotating speed, the pump mass flow rate increases rapidly, while the isentropic efficiency increases first and then decreases. As shown in Figure 11, the exhaust entropy increase is the smallest at 10000 rpm, and the isentropic efficiency reaches the maximum at the design speed. Figure 12 shows the radial clearance leakage velocity at different speeds. With the increase of rotating speed, the clearance leakage velocity increases obviously due to the same rotation direction of the co-rotating scroll with the radial clearance leakage flow. For the co-rotating scroll pump, the clearance leakage under high rotating speed should be paid attention and reduced by suitable sealing method.

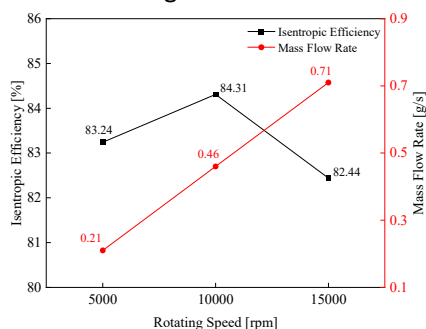


Fig. 10. Isentropic efficiency at different speeds

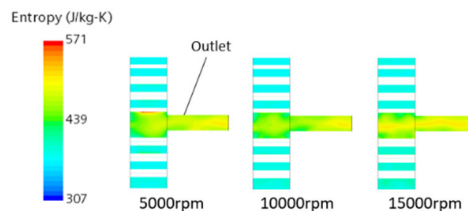


Fig. 11. Exhaust entropy at different speeds

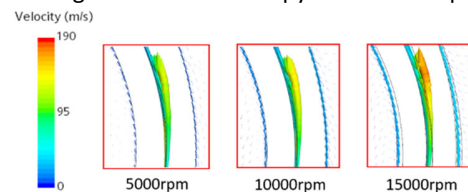


Fig. 12. Clearance leakage velocity at different speeds

As shown in Figure 13, with the increase of rotating speed, the maximum pressure at the end of compression increases. The maximum pressure of over-compression at 10000 rpm increases by 12kpa compared with 5000 rpm.

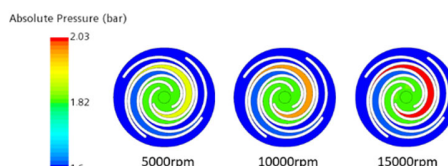


Fig. 13. Over compression at different speeds

#### 4.3 Effect of hydrogen humidity

##### 4.3.1 Effect of hydrogen humidity on Performance

The mass fraction of hydrogen and water vapor and volume flow rate under different humidity are shown in Table 3. Figure 14 shows the isentropic efficiency under different hydrogen humidity. The isentropic efficiency of the hydrogen recirculation pump is greater than 80%, but it decreases with the hydrogen humidity. The isentropic efficiency under 100% hydrogen humidity decreases by about 2.3% compared with dry hydrogen. As shown in Figure 15, with the increase of hydrogen humidity, the temperature rise at the inlet and outlet gradually increases, while the pressure rise gradually decreases. The maximum difference is about 0.3K and 0.62Kpa, respectively.

Humidity %	Mass Fraction Hydrogen: Water	Volume Flow Rate L/min
0	1:0	247.99
20	0.67:0.33	249.46
60	0.375:0.625	251.53
100	0.24:0.76	252.73

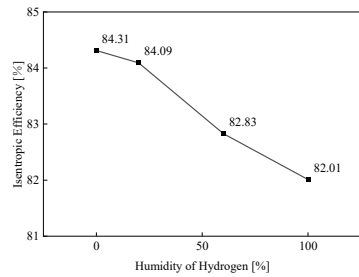


Fig. 14. Isentropic efficiency under different humidity

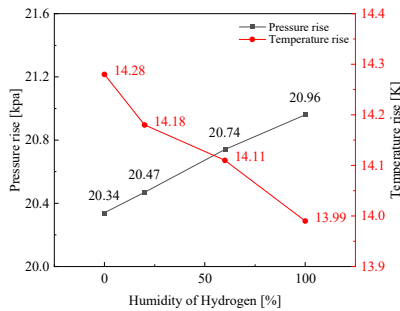


Fig. 15. Pressure and temperature rise under different hydrogen humidity

#### 4.3.2 Effect of hydrogen humidity on the flow field

The existence of water vapor has an apparent influence on the pressure and velocity field. As shown in Figure 16 (a), with the increase of humidity, the mass proportion of water vapor and the density increase. As a result, the highest pressure of over-compression in the compression chamber rises at the end of compression. Compared with dry hydrogen, the maximum hydrogen pressure under 100% humidity increased by about 4Kpa. A local relatively low-pressure area appears at the central discharge chamber, while the central pressure is relatively uniform under dry hydrogen conditions, as shown in Figure 16 (b).

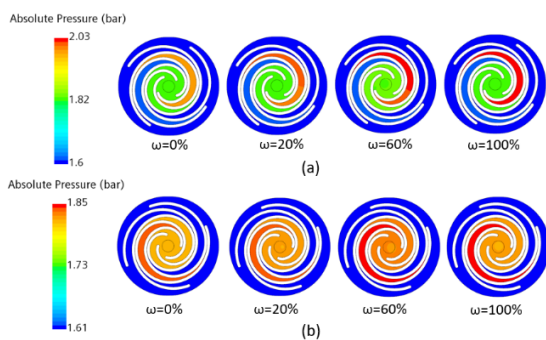


Fig. 16. Pressure distribution under different humidity

As shown in Figure 17 (a) and (b), the velocity and Mach number distributions are similar under different hydrogen humidity. The maximum velocity and Mach number occur at the radical clearance. With the increase of hydrogen humidity, the maximum flow rate at the radical clearance decreases, while the Mach number at

the inlet and central discharge chamber gradually increase.

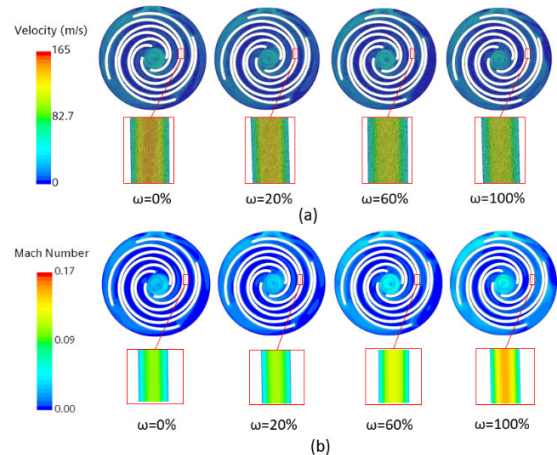


Fig. 17. Velocity distribution under different humidity: (a) Velocity, (b) Mach Number

## 5. CONCLUSION

To realize the compactness and lightweight of the hydrogen recirculation pump, the basic parametric design of a co-rotating hydrogen recirculation pump with two pairs of scrolls and numerical simulation under different hydrogen humidity were carried out. The main conclusions were as follows:

(1) The flow field distribution of co-rotating scroll hydrogen recirculation pump may be different from that of orbiting due to the different motion modes of scrolls. The fluid in the compression chamber is in a low-speed flow state, while the fluid velocity close to the scroll wall is relatively fast. The velocity distribution at the inlet of the suction chamber and the outlet of the exhaust chamber are uniformly affected by the inlet high-speed fluid or pressure gradient;

(2) Affected by the rotation of two pairs of scrolls, the turbulence at the inlet of the suction chamber and central exhaust chamber is more intense, resulting in four peaks of inlet and outlet mass flow in a rotation revolution, and the pulsation of exhaust mass flow is significantly more intense.

(3) The over-compression of gas and exhaust loss become more serious at high speed because of the rapid increase of suction capacity, which leads to the decrease of isentropic efficiency. The increase of rotating speed will aggravate the gap leakage because the rotation direction of scrolls is consistent with the leakage flow direction of radial clearance.

(4) With the increase of hydrogen humidity, the isentropic efficiency of hydrogen recirculation pump decreases, as well as the temperature. The pressure rise between the inlet and outlet port increases When the

hydrogen humidity is 100%, the isentropic efficiency decreases by about 2.3%. The maximum difference of pressure rise and temperature rise is 0.63Kpa and 0.3k respectively.

(5) Different humidity has a certain influence on the flow field characteristics. As the hydrogen humidity increases to 100%, the gap flow velocity decreases by about 30m/s. The maximum Mach number gradually increases to 0.17.

#### ACKNOWLEDGEMENT

This work was supported by the National Natural Science Foundation of China (Grant No.51906015).

#### REFERENCE

- [1] Xing, L., He, Y., Wen, J., & Peng, X. (2018). Three-dimensional CFD Modelling of a Roots Blower for Hydrogen Recirculation in Fuel Cell System.
- [2] Liu Kai. Construction of a new rotor profile and working characteristics of claw-type machinery characteristics [D]. China University of Petroleum, 2013
- [3] Luo Nan, Zhang Shixing, Zheng Tianyi. Research on performance of centrifugal compressor [J]. Chemical equipment technology, 2020,41 (06): 59-62
- [4] WANG, J., JU, H., ZHAO, M., & QU, Y. (2009). Influence of wrap number on performance of multi-wrap scroll compressor [J]. Journal of China University of Petroleum (Edition of Natural Science), 3.
- [5] Li Chao, Liu Zhenquan, Wang Jun. research on oil-free scroll compressor for fuel cell [J]. Lubrication and sealing, 2008 (06): 74-76 + 92
- [6] HUANG, Y., LI, J. J., HAN, J. X., & ZHANG, Y. C. (2013). Development and key problems of the dry scroll vacuum pump. Vacuum, 03.
- [7] Zhou Jiasheng. Revolution and rotation scroll fluid machinery [J]. Compressor technology, 1997 (05): 10-11 + 36
- [8] Olmedo, L. E. , Mounier, V. , Mendoza, L. C. , & Schiffmann, J. . (2018). Dimensionless correlations and performance maps of scroll expanders for micro-scale organic rankine cycles. Energy, 156(AUG.1), 520-533.
- [9] Toledo, L. C. M. , & Jürg Alexander Schiffmann. (2014). Experimental Investigation of Water Injection in an Oil-Free Co-Rotating Scroll Machinery for Compressed Air Energy Storage. Purdue Conferences, Compressor Engineering.
- [10] Favrat, D., Iglesias, & A. (2014). Innovative isothermal oil-free co-rotating scroll compressor-expander for energy storage with first expander tests. Energy conversion & management, 85(Sep.), 565-572.
- [11] Mendoza, L. C. , Lemofouet, S. , & Schiffmann, J. . (2017). Testing and modelling of a novel oil-free co-rotating scroll machine with water injection. Applied Energy, 185(pt.1), 201-213.
- [12] Shaffer, R. W., Shaffer, B. R., & Vigil, R. (2020). U.S. Patent No. 10,683,865. Washington, DC: U.S. Patent and Trademark Office.
- [13] Wilson, J. P., & Nicholas, N. D. (2020). U.S. Patent Application No. 16/514,639.